

Cosmic Phase Transitions as a source of Gravitational Waves

Karishma M.

May-August 2019

1 Introduction

During my co-op term at TRIUMF in the Summer of 2019, I worked on Cosmic Phase transitions in the Early Universe, and the gravitational waves that possibly resulted from these phase transitions. This was under the supervision of David Morrissey and Djuna Croon.

The goal is to develop a theory that answers some of the questions we have, with our present understanding of the Standard Model, and be able to verify this theory through search and observation of gravitational waves. The hope is that the gravitational waves predicted from such a theory, would be within the sensitivity of present-day detectors... or at least, of those that will be active in the near future.

The road map of this effort is shown in the flow-chart below:

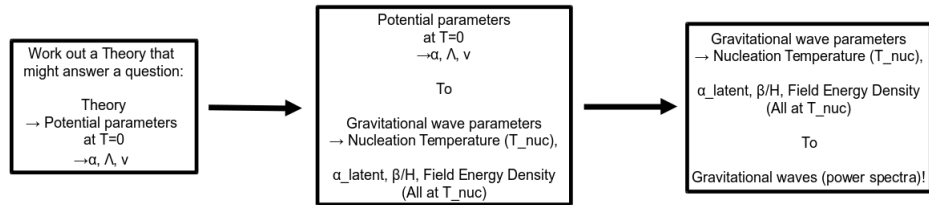


Figure 1: Three stages in getting from Theory till Observable data

Note: The theory is set in the time period between inflation and the QCD phase transition; hence our expression for the Hubble rate is based on a **radiation-**

dominated Universe.

My work this term, was developing code that will be able to perform all the required Physics and Math in Stage 2. To do so, I first analyzed the WKB approximation for a specific kind of potential, to gain intuition for how the system would work. Then, I moved on to the Bubble approximation (also known as the Instanton Solution) to perform the main calculations and develop a method in Python, that quickly does Stage 2 of the flow-chart for the user.

Refer Appendix for the WKB approximation.

————— x ————— x —————

2 The Bubble/Bounce Approximation - General method

The goal to find the tunneling rate of some field from false vacuum to true vacuum i.e. the rate at which it tunnels across the potential barrier and therefore, undergoes a first-order phase transition.

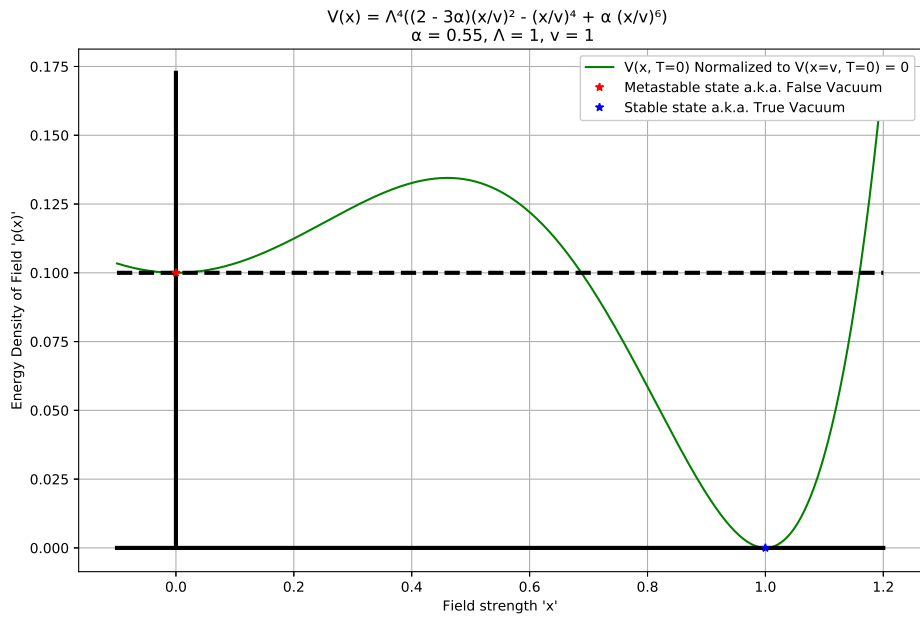


Figure 2: Potential with 2 vacua; field tunnels from metastable state to stable state

On attempting to solve for a scalar field, we work with the potential (in Minkowski space i.e. real space), $V_{Minkowski}(\phi)$, where ϕ is the function for the scalar field.

A Wick Rotation was performed, taking the problem to the Euclidean space:

$$V_{Euclidean}(\phi) = -V_{Minkowski}(\phi)$$

$$S_{Euclidean}[\phi] = -iS_{Minkowski}[\phi]$$

Now, the field Lagrangian of the scalar field, $\mathcal{L}[\phi(\vec{x}), \dot{\phi}(\vec{x})]$,

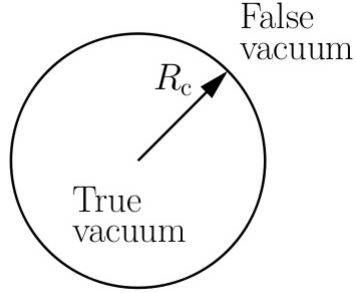


Figure 3: Bubble of true vacuum expanding into false vacuum [6]

$$\mathcal{L}[\phi(\vec{x}), \dot{\phi}(\vec{x})] = \frac{1}{2}(\nabla\phi)^2 - V_{Euclidean}(\phi);$$

where $\phi(\vec{x})$ is the field that can describe the behaviour of the particle/interaction

Also, it is known that:

$$S_{D, Euclidean} = \int \mathcal{L}[\phi(\vec{x}), \dot{\phi}(\vec{x})].d^D\vec{x}$$

where S is the Euclidean action.

The Euler-Lagrange E.O.M. is applied, assuming spherical symmetry i.e. $\phi(\rho)$, where $\rho = \sqrt{x_1^2 + x_2^2 + \dots + x_D^2}$.

This gives us:

$$\frac{d^2\phi}{d\rho^2} + \frac{(D-1)}{\rho} \frac{d\phi}{d\rho} + \frac{dV_{Euclidean}}{d\phi} = 0$$

— Main O.D.E.

where boundary conditions are $\frac{d\phi}{d\rho}|_{\rho=0} = 0$; $\phi(\rho = \infty) = 0$

The above assumptions stem from the fact that the transition from metastable to stable state is a first order phase transition and so it forms a bubble of true vacuum that expands across the false vacuum until the entire D-space is in the state of true vacuum. Bubble \Rightarrow spherical symmetry. Since the lowest energy state of the field starts in the metastable vacuum and ends at some energy level in the stable vacuum, the boundary conditions are applied as shown.

We attempt to solve this for $D = 3$ and $D = 4$.

$D = 3$ implies that here it is assumed that Temperature acts as a scale of Time; $\rho = \sqrt{x^2 + y^2 + z^2}$. This is the case when tunneling is caused by thermal fluctuations

$$\text{Tunneling Probability} \sim e^{-S_{\text{Euclidean}}/T}$$

$D = 4$, includes Time in ρ ; $\rho = \sqrt{x^2 + y^2 + z^2 + t^2}$ ($c = 1$); This is the case when tunneling is caused by quantum fluctuations in the vacuum.

$$\text{Tunneling Probability} \sim e^{-S_{\text{Euclidean}}}$$

Refer Figure 15 (in Appendix) to see different types of potentials leading to different types of the bounce/instanton solutions, $\phi(\rho)$.

Once $\phi(\rho)$ is found, the Euclidean action is calculated:

For $D = 3$:

$$\begin{aligned} S_{\text{Euclidean}} &= \int [(\frac{d\phi}{d\rho})^2 - V_{\text{Euclidean}}(\phi)] d^3x \\ &= \int \int \int [(\frac{d\phi}{d\rho})^2 - V_{\text{Euclidean}}(\phi)] \rho^2 \sin(\theta) d\rho d\theta d\psi \\ \Rightarrow S_{\text{Euclidean}}[\phi(\rho)] &= 4\pi \int [(\frac{d\phi}{d\rho})^2 - V_{\text{Euclidean}}(\phi(\rho))] \rho^2 d\rho \end{aligned}$$

Similarly, for $D = 4$:

$$\Rightarrow S_{\text{Euclidean}}[\phi(\rho)] = 4\pi^2 \int [(\frac{d\phi}{d\rho})^2 - V_{\text{Euclidean}}(\phi(\rho))] \rho^3 d\rho$$

NOTE: Due to computational limitations, the thin wall approximation was used to calculate the action at times.

From here, the tunneling rate and other gravitational wave parameters are calculated, with the equations below:

Tunneling probability per unit Hubble volume, ...[5][1]

$$\text{For } D = 3, \frac{\Gamma}{V}(T) = T^4 e^{-S_3/T}$$

$$\text{For } D = 4, \frac{\Gamma}{V}(T) = T^4 e^{-S_4}$$

$$\text{where, } V = \frac{1}{H^3}$$

$$\text{Hubble Rate} = H = \pi \sqrt{\frac{g_*}{90}} \frac{T^2}{M_{\text{Planck}}} \text{ (assuming } \alpha_{\text{latent}} \ll 1 \text{)} \quad \dots[4]$$

Nucleation temperature is also found: nucleation temperature is the temperature at which the tunneling rate is equal to the Hubble rate. As temperature

decreases, the tunneling rate increases beyond the Hubble rate i.e. the formation and expansion rate of the bubbles can catch up to and overtake the expansion of the Universe.

$$\Gamma(T_{Nucl}) = H(T_{Nucl}) \quad \dots [5]$$

Apart from nucleation temperature, the other parameters required for finding the gravitational wave spectra are "latent heat" and "nucleation rate" [5].

Latent heat (i.e. phase transition strength) is given by:

$$\alpha_{latent} = \frac{\Delta\rho_\phi}{\rho_{rad}}|_{atT_{Nucl}} \quad \dots [5]$$

$$\text{where, } \rho_{rad} = \pi^2 \frac{g_*(T)}{30} T^4 \quad \dots [5]$$

$$\text{and } H^2 = \frac{1}{3M_P^2} \rho_\phi \quad \dots [4]$$

It is necessary that $\alpha_{latent} < 1$, because otherwise, our assumptions about the Hubble rate (and hence the location of the nucleation temperature) fall apart. The assumption implies that the overall contribution of the field in question is much less than the background radiation at that temperature. Basically, α_{latent} is a measure of the energy density of the field before the phase transition, as compared to that of all the other radiation... and so, as mentioned earlier, is a measure of phase transition strength (higher energy release \Rightarrow stronger phase transition) [5]

Lastly, the nucleation rate (also known as the "inverse phase transition duration") is found:

$$\frac{\beta}{H} = T \frac{dS}{dT}|_{atT_{Nucl}}$$

$$\text{where } S \text{ for } D = 3, \text{ is } \frac{S_3}{T}$$

$$\text{and } S \text{ for } D = 4, \text{ is } S_4 \quad \dots [5]$$

3 The Problem at hand and how it was dealt with

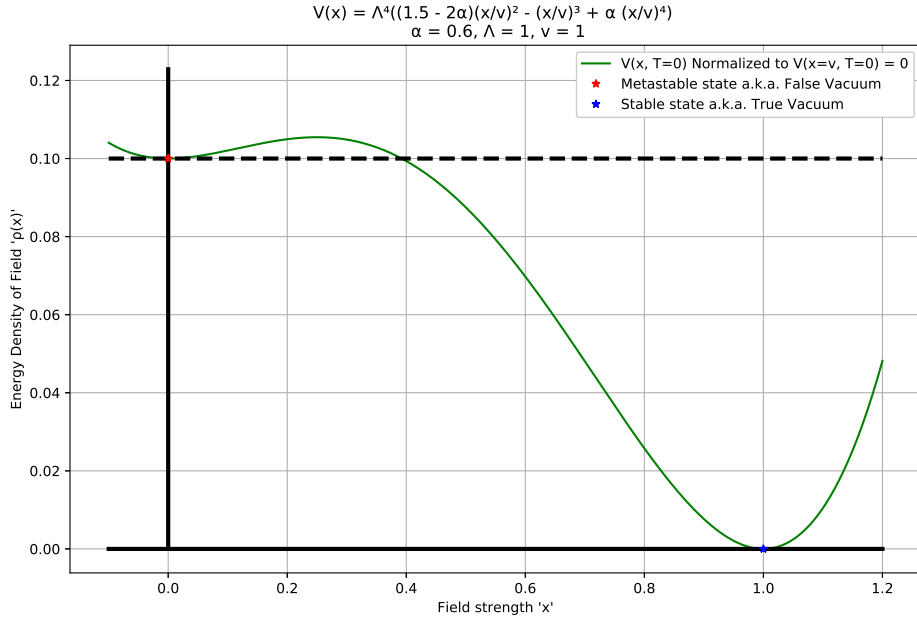


Figure 4: Potential with 2 vacua; field tunnels from metastable state to stable state

Here, we have:

$$V_{Minkowski}(\phi) = \mu^2 \phi^2 - A \phi^3 + \lambda \phi^4 \quad \text{— Eqn. 1}$$

This (Eqn. 1) is the zero-temperature potential - it defines the field theory we are working with. Over the course of time, the potential actually varies with the decreasing temperature, given by:

$$V_{Minkowski}(\phi, T) = (\mu^2 + T^2) \phi^2 - A \phi^3 + \lambda \phi^4 \quad \text{— Eqn. 2}$$

where, T is the temperature, and Eqn. 1 is the $T = 0$ potential i.e. the (potential of the) theory we are working with.

For the sake of convenience, μ is redefined as μ_{eff} , to give:

$$V_{Minkowski}(\phi, T) = \mu_{eff}^2 \phi^2 - A\phi^3 + \lambda\phi^4$$

— Eqn. 3

where, $\mu_{eff} = \sqrt{\mu^2 + T^2}$

](**Note:** Henceforth, whenever the subscript "eff" is used, it implies that the parameter is temperature dependent.)

The goal is to calculate action $S_{Euclidean}$ (and consequently, tunneling rate) as a function of temperature T .

We want to express this 2-3-4 polynomial (and other potentials, when possible e.g. 2-4-6 potentials) as:

$$V_{Minkowski}(\phi, T) = \Lambda_{eff}^4 \cdot ((\dots) \cdot (\frac{\phi}{v_{eff}})^2 - (\frac{\phi}{v_{eff}})^3 + \alpha_{v,eff} \cdot (\frac{\phi}{v_{eff}})^4)$$

This parametrization is particularly useful, as Λ is defined to be the quantity that holds the dimensions of the potential and thereby act as the general energy scale of the potential. Also, v is defined as the field strength such that the energy density of field, at $\phi = v$, is the Vacuum Expectation Value (VEV) of the field (It is assumed that VEV of field is basically 0 today). And finally, α_v is defined as the parameter that determines the specific shape of the potential (in regards to the definition of the 2 potential wells). It is purely dimensionless - so the skeleton of the problem can be based on how things vary with α_v .

So to find the (\dots), which specific to the potential itself, $V_{Minkowski}(\phi)$ was differentiated w.r.t. ϕ ; and it was noted that $V'_{Minkowski}(\phi = v) = 0$, by definition of 'v' (since 'v' is a local minimum). This resulted in:

$$\begin{aligned} V'_{Minkowski}(\phi, T) &= \frac{\Lambda_{eff}^4}{v_{eff}} \cdot (2(\dots) \cdot (\frac{\phi}{v_{eff}}) - 3(\frac{\phi}{v_{eff}})^2 + 4\alpha_{v,eff} \cdot (\frac{\phi}{v_{eff}})^3) \\ \Rightarrow V'_{Minkowski}(v, T) &= \frac{\Lambda_{eff}^4}{v_{eff}} \cdot (2(\dots) \cdot (1) - 3(1)^2 + 4\alpha_{v,eff} \cdot (1)^3) = 0 \\ \Rightarrow 2(\dots) - 3 + 4\alpha_{v,eff} &= 0 \\ \Rightarrow (\dots) &= \frac{3-4\alpha_{v,eff}}{2} \end{aligned}$$

Therefore:

$$V_{Minkowski}(\phi, T) = \Lambda_{eff}^4 \cdot ((\frac{3-4\alpha_{v,eff}}{2}) \cdot (\frac{\phi}{v_{eff}})^2 - (\frac{\phi}{v_{eff}})^3 + \alpha_{v,eff} \cdot (\frac{\phi}{v_{eff}})^4)$$

— Eqn. 4

A constant is added to $V_{Minkowski}(\phi, T)$, so as to get the energy density of the field at $T = 0$ i.e., the potential must be normalized, such that $V(\phi = v, T = 0) = 0$. So, we define:

$$V(\phi, T) = \Lambda_{eff}^4 \cdot \left(\left(\frac{3-4\alpha_{v,eff}}{2} \right) \cdot \left(\frac{\phi}{v_{eff}} \right)^2 - \left(\frac{\phi}{v_{eff}} \right)^3 + \alpha_{v,eff} \cdot \left(\frac{\phi}{v_{eff}} \right)^4 \right) + \Lambda^4 (\alpha_v - \frac{1}{2}) \quad \text{— Eqn. 5}$$

Comparing this with Eqn. 3 we have:

$$v = \frac{3A + \sqrt{9A^2 - 32\mu_{eff}^2 \lambda}}{8\lambda}$$

$$\alpha_v = \frac{\lambda v}{A}$$

$$\Lambda^4 = A \cdot v^3$$

All the quantities above have dimensions.

In Natural units $\hbar = c = k_B = 1$,

$$[\phi] = E, [\rho] = E^{-1},$$

$$[\mu] = E, [A] = E, [\lambda] = 1,$$

$$[\Lambda] = E, [v] = E, [\alpha_v] = 1,$$

$$[V] = E^4$$

$$[T] = E$$

and

$$[S] = E \text{ (when } D = 3 \text{) and } 1 \text{ (when } D = 4 \text{)}$$

where E holds the dimensions of energy.

To have a system that does not have it's basic design (like, for example, the location of "infinity", or the basic shape of the curve) depending on these parameters, dimensionless quantities must be used.

Hence, a transformation that *conveniently* makes everything dimensionless (to solve the equation), and then allows us to return the dimensions to the problem (so that solution is not affected by energy scale of problem) was used.

So, the following transformation was done:

$$\phi = \frac{\phi_{dimensionful}}{v}$$

$$V = \frac{V_{dimensionful}}{\Lambda^4}$$

This makes things way more convenient.

Observing Eqn. 2, note that μ and T have the same dimensions. Also note that, to maintain the above transformations, T (and also μ) must transform as:

$$T = T_{dimensionful} \frac{v}{\Lambda^2}$$

Now, it is known that:

$$S_{Euclidean}[\phi(\rho)] = k \int [(\frac{d\phi}{d\rho})^2 - V_{Euclidean}(\phi(\rho))] \rho^{D-1} d\rho$$

We want a transformation: $S_{dimensionful} \rightarrow S$, such that:

$$S = (\text{scalar}).S_{dimensionful}$$

So, the same factor must be pulled out from both $(\frac{d\phi}{d\rho})^2$ and $V_{Euclidean}(\phi(\rho))$. Since the transformations for V and ϕ are already known, the corresponding transformation for ρ is found to be:

$$\rho = \rho_{dimensionful} \frac{\Lambda^2}{v}$$

And therefore,

$$S = \frac{1}{\Lambda^4} \left(\frac{\Lambda^2}{v} \right)^D S_{dimensionful}$$

So,

$$\text{For } D = 3, \dots, S = \frac{\Lambda^2}{v^3} S_{dimensionful}$$

$$\text{and so, } S/T = \left(\frac{\Lambda}{v} \right)^4 (S/T)_{dimensionful}$$

and

$$\text{For } D = 4, \dots, S = \left(\frac{\Lambda}{v} \right)^4 S_{dimensionful}$$

And using this action, the tunneling rate is found.

Refer Section 2 for all the other relevant formulae.

4 The Solutions found for a Specific Theory

$$\text{Example shown: } V_{T=0}(\phi) = 1000^4 \left(0.3\left(\frac{\phi}{1000}\right)^2 - \left(\frac{\phi}{1000}\right)^3 + 0.6\left(\frac{\phi}{1000}\right)^4\right)$$

i.e. Theory is given by 2-3-4 Potential, with: $\alpha_v = 0.6$, $\Lambda = 1000$ GeV, $v = 1000$ GeV

The above defines our T=0 potential... which, in turn, can tell you how the energy density/potential of the field varies with temperature, throughout the process.

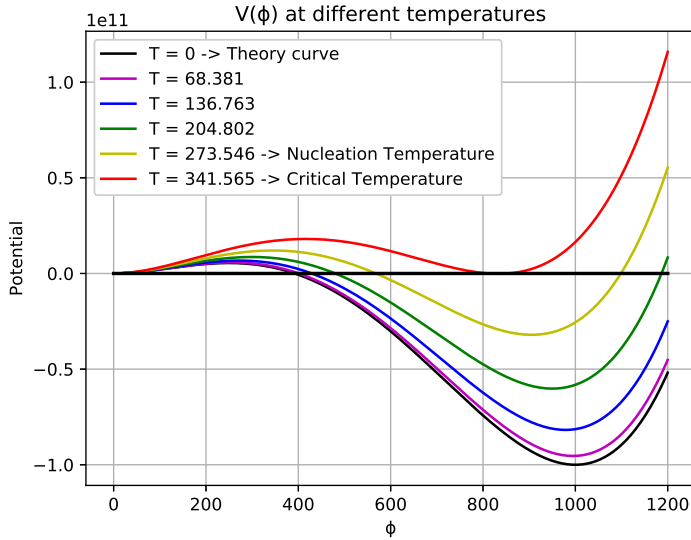


Figure 5: Potential varying with Temperature; Note that Nucleation temperature is only for D=3. See Figure 8

So the potential is made dimensionless i.e. $\Lambda \rightarrow 1$ and $v \rightarrow 1$. And then, $\phi(\rho)$ is solved for, using the equation found in Section 2.1, using the shooting method.

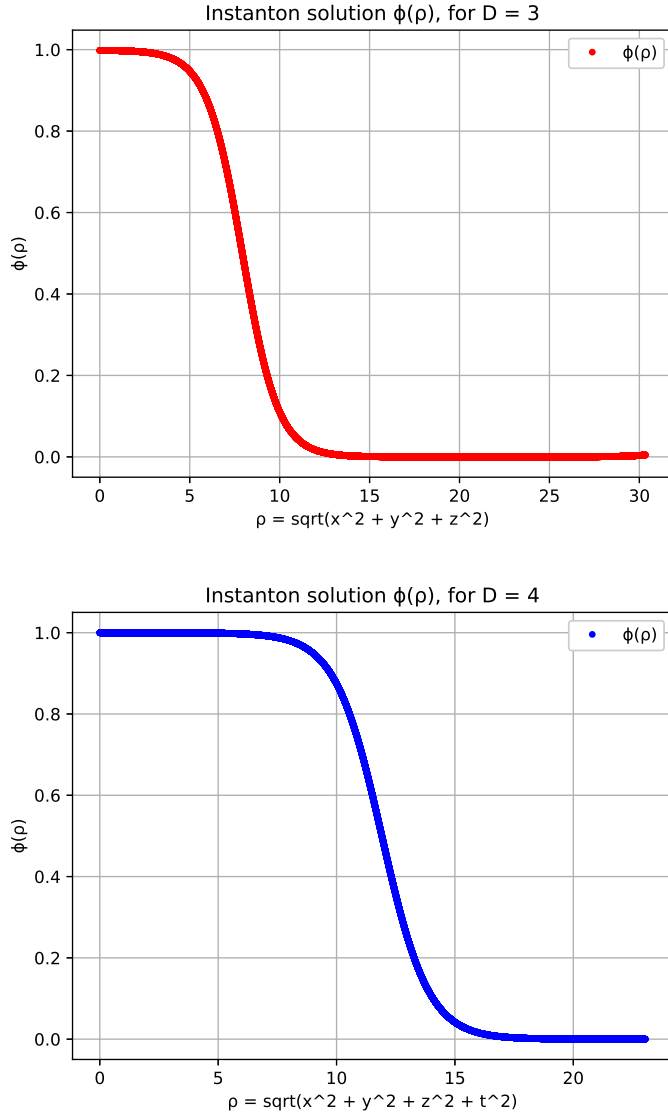


Figure 6: Instanton Solution for $\alpha_{eff} = 0.543$ i.e. $T = 273.546$ GeV; for both $D=3$ and $D=4$

Solutions like the above cannot be found all the time. Usually in cases where the potential wells are near degenerate, $\phi(\rho)$ cannot be found exactly. In those cases, either the thin wall approximation is applied to directly find the action, or a curve fit/interpolation is performed between the actions of the thin wall region, and the actions where the solution could be found exactly.

Now that $\phi(\rho)$ was found for a specific α_{eff} , the action for that specific α_{eff} was found. This was repeated for all possible α_{eff} to create the S vs. α_{eff} template, so as to make the process quicker: refer Figure 9.

Now the factor of $(\frac{v}{\Lambda})^4$ is multiplied to the dimensionless action we found, to create the Action as a function of Temperature, for the theory we're working with. This Action was found for all values between $T_{critical}$ and $T=0$.

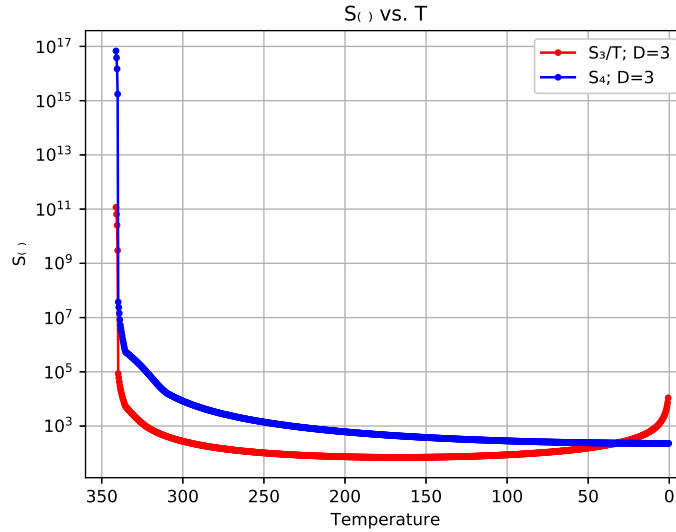


Figure 7: S_3/T and S_4 as a function of Temperature

Then, using formulae shown in Section 2, the tunneling rate, the Hubble rate and the parameters required to produce gravitational wave power spectra for the given theory, were found.

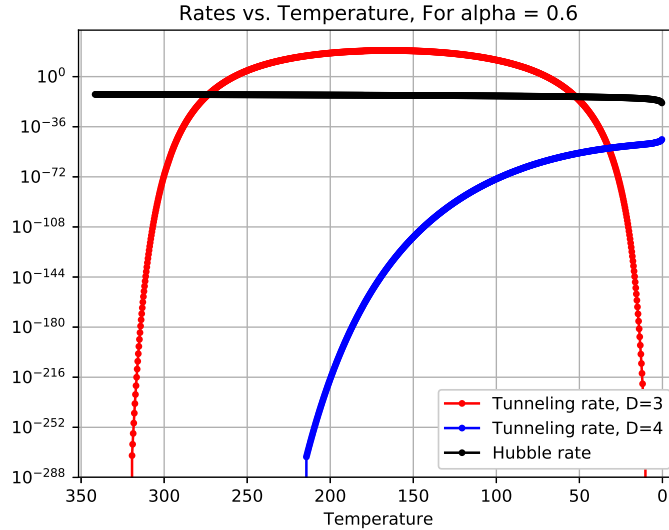


Figure 8: Tunneling rate crossed Hubble rate for $D=3$ and hence nucleation can occur (the temperature at which the rates cross: $T_{Nucleation} = 273.546$ GeV). For $D=4$, nucleation cannot occur because tunneling rate can never cross the Hubble rate.

From analyzing the above plot, it is seen that the thermal fluctuations lead to nucleation at about 273.55 GeV, with $\alpha_{latent} = 0.16$ and $\beta/H = 688.02$. The quantum fluctuations never lead to nucleation in this theory.

In general, quantum fluctuations never lead to nucleation before the thermal fluctuations. And since the bubbles form pretty quickly, the quantum fluctuations never get involved in the nucleation process, and hence they are ignored henceforth.

Hence, for a given theory α_v , Λ and v , gravitational wave power spectra parameters $T_{Nucleation}$, α_{latent} and β/H are found.

5 The General Trends for 2-3-4 Potentials

First let's outline the skeleton of this family of potentials. See below the graphs for Dimensionless action vs. α_v . Note: Dimensionless implies setting $\Lambda = v = 1$ (and re-scale later).

Points of Note regarding Figure 9:

1. In the region where $0.506 < \alpha_v < 0.520$, notice the graph is not smooth (especially evident in D=4). This is a direct result of the fact that Coleman's thin wall approximation could not be applied here, and neither could the exact analytic solution $\phi(\rho)$ be found. So 'Piece-wise Cubic Hermite Interpolating Polynomial' (PCHIP Interpolation) was used to connect the 2 regions.
Also note that the graph looks a lot smoother when zoomed in -> again, makes sense since the curve fit was done by polynomials.
2. In the region of α_v very close to 0.5, it is expected that S will asymptotically tend towards infinity. But that is not evident.

To elaborate on the 2nd point: S was not calculated for $\alpha_v = 0.5$ (and only near it), because at $\alpha_v \rightarrow 0.5$, $S \rightarrow \infty\dots$ which is not manageable computationally. So we did not go past $\alpha_v < 0.500001$: the PCHIP Interpolation was used to approximate the behaviour past that threshold. This explains the curve there. But the sudden jump around $\alpha_v \leq 0.5015$ is unexplained. We think that, that jump is due to the computational limitations caused by the fact $R \rightarrow \infty$ in the Coleman approximation... but this has not been verified. Regardless, **it is assumed that the code is unreliable past $\alpha_v \leq 0.5015$**

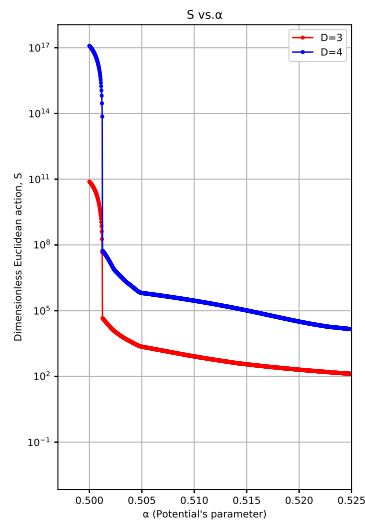
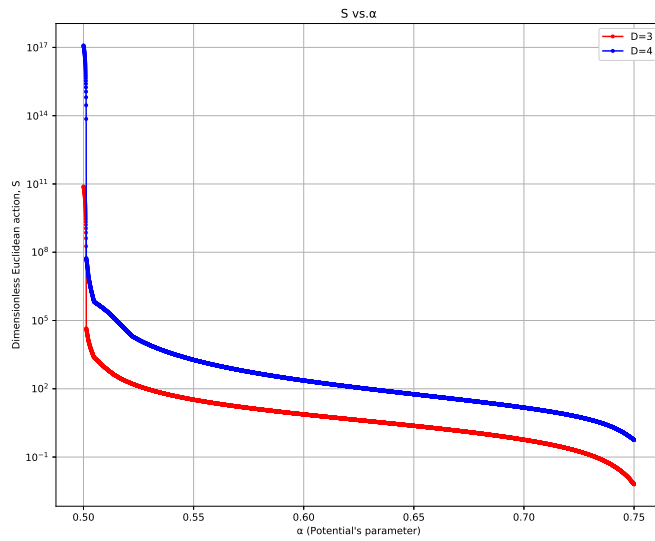


Figure 9: Dimensionless Euclidean Action as a function of dimensionless parameter of generic 2-3-4 Potential (i.e. $\Lambda = v = 1$)

From here, using the expressions outlined in Section 2.1, β/H and α_{latent} are found, for different kinds of quartic potentials (based on the parametrization shown in Section 3).

The following plots have been made for $\alpha_v \in \{0.51, 0.54, 0.57, 0.6, 0.64, 0.65, 0.68, 0.72, 0.75, 0.78, 0.81\}$; If a point has not been plotted, the reasons will be explained in the observations below.

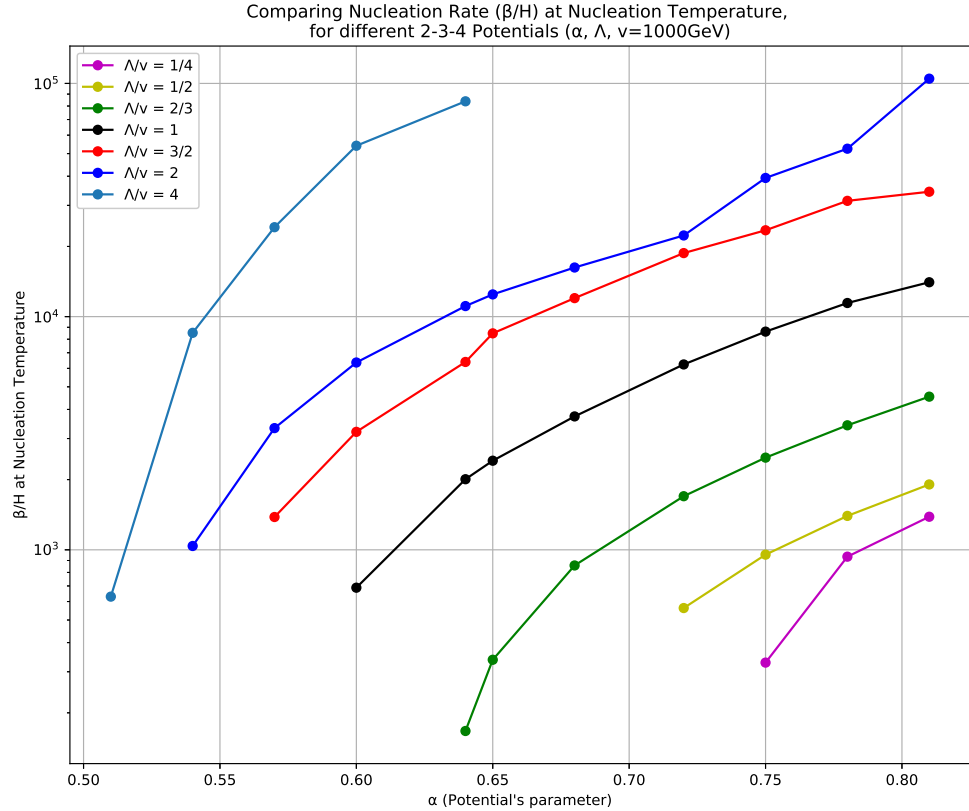


Figure 10: $\frac{\beta}{H}$ vs. α_v (of T=0 Potential parameter)

Observations based on Figure 10:

1. Potentials where $\Lambda = v$, have $\frac{\beta}{H}$ not defined for $\alpha_v \leq 0.57$, because tunneling rate can never catch up to Hubble rate.
2. As the $\frac{\Lambda}{v}$ ratio increases, more α_v values allow tunneling rate to catch up

to Hubble rate. This is because when $\frac{\Lambda}{v}$ is high, the energy released on undergoing transition is high... even when the vacua are closer to being degenerate. Hence tunneling is more favorable and tunneling rate can easily catch up to Hubble rate. Also note that as $\frac{\Lambda}{v}$ increases, so does the overall magnitude of $\frac{\beta}{H}$ (nucleation rate) increases.

- When $\frac{\Lambda}{v} \gg 1$, the graph does not go beyond $\alpha_v \geq 0.65$ or so. This is because of very intense supercooling, which results in nucleation temperature being at a temperature where $\alpha_v \leq 0.5015 \Rightarrow$ in the region of theoretical uncertainty.

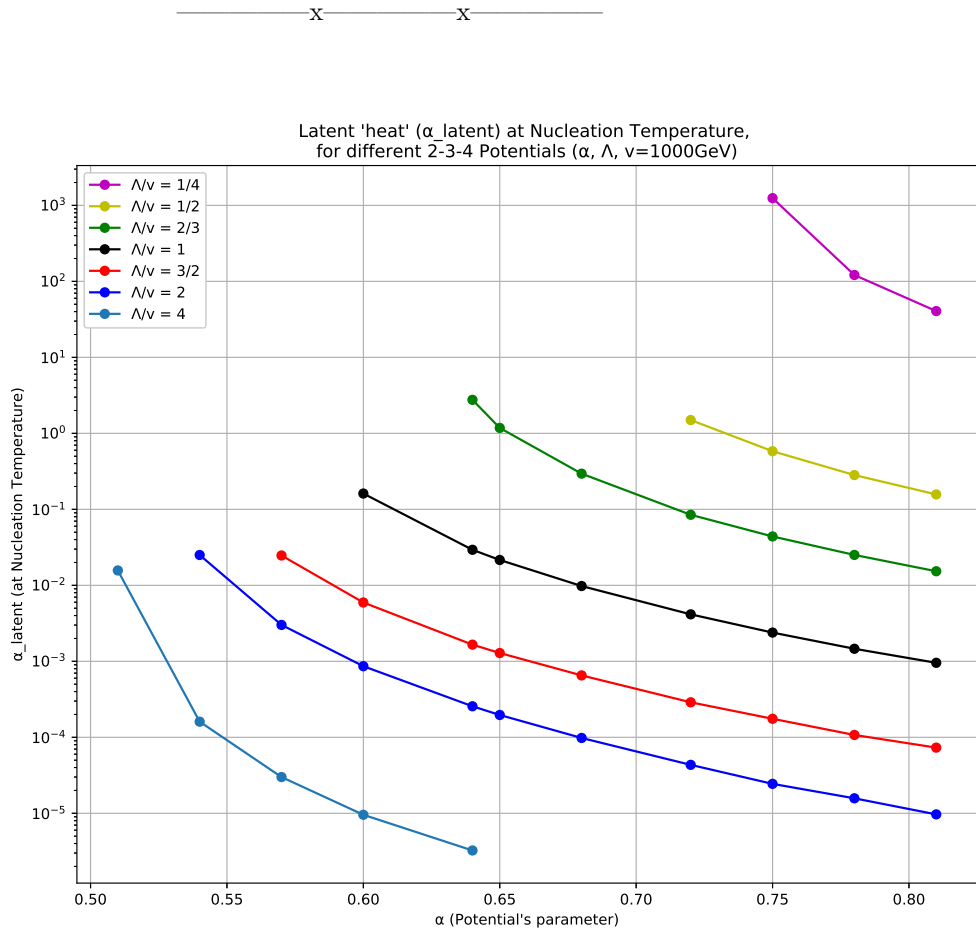


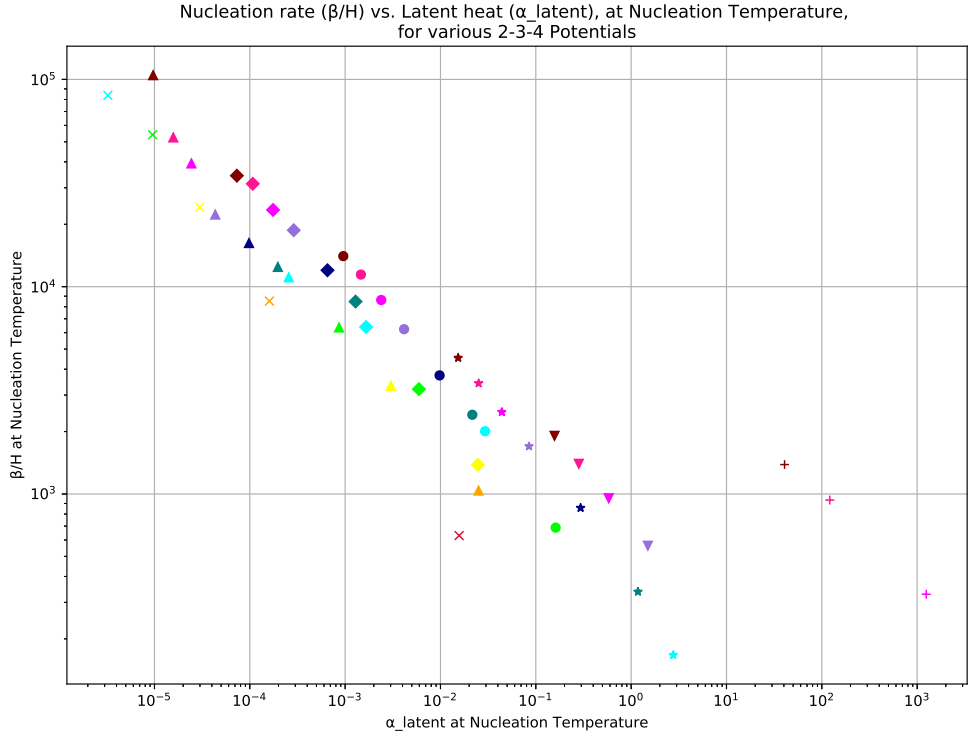
Figure 11: α_{latent} vs. α_v (of T=0 Potential parameter)

Observations based on Figure 11:

1. Potentials where $\Lambda = v$, have α_{latent} not defined for $\alpha_v \leq 0.57$, because tunneling rate can never catch up to Hubble rate... so there is no Nucleation temperature for α_{latent} to even be defined.
2. As the $\frac{\Lambda}{v}$ ratio increases, more α_v values allow tunneling rate to catch up to Hubble rate. Same reasoning as in the 'Observations based on Figure 10'.
3. As $\frac{\Lambda}{v}$ increases, the overall magnitude of α_{latent} decreases. This means, the contribution of field ϕ to overall radiation energy density is lower, meaning our expression for Hubble rate (and hence nucleation temperature) is more accurate in this region.
4. Refer Obs. 3 of 'Observations based on Figure 10'

It is required that $\alpha_{latent} < 1$. So ALL the theories where $\frac{\Lambda}{v} = \frac{1}{4}$ have to be discarded. And, in general, **when $\frac{\Lambda}{v} < 1$, the lower values of α_v must be discarded.**

————— x ————— x —————



α_v Values	Colour Code	Λ/v Values	Symbol Code
0.51	Red	$\Lambda/v = 1/4$	Plus
0.54	Orange	$\Lambda/v = 1/2$	Downward triangle
0.57	Yellow	$\Lambda/v = 2/3$	Star
0.6	Green	$\Lambda/v = 1$	Circle
0.64	Cyan	$\Lambda/v = 3/2$	Diamond
0.65	Teal Blue	$\Lambda/v = 2$	Upward triangle
0.68	Navy Blue	$\Lambda/v = 4$	Cross
0.72	Indigo		
0.75	Fuchsia		
0.78	Pink		
0.81	Brown		

$v = 1000 \text{ GeV}$

Figure 12: $\frac{\beta}{H}$ vs. α_{latent} for different $T=0$ Quartic Potentials

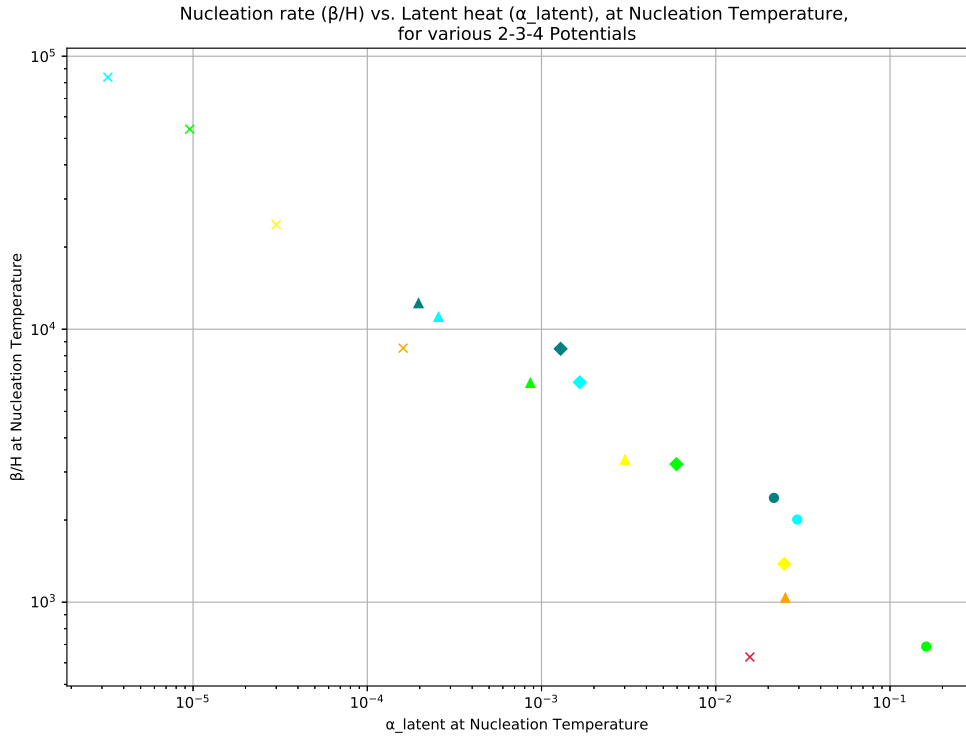
Observations based on Figure 12:

1. Potentials where $\Lambda = v$, have α_{latent} and $\frac{\beta}{H}$ not defined for $\alpha_v \leq 0.57$ (i.e. you can't see Yellow, Orange and Red Circles) \rightarrow refer previous Observations.
2. As the $\frac{\Lambda}{v}$ ratio increases, more α_v values allow tunneling rate to catch up to Hubble rate. Same reasoning as in previous Observations. Also

note that as $\frac{\Lambda}{v}$ increases, the overall magnitude of α_{latent} decreases and $\frac{\beta}{H}$ increases i.e. towards the top left corner of the graph.

Gravitational waves produced by sources towards the bottom right corner of the graph, in general, are within the sensitivity of modern day detectors/detectors in the foreseeable future (like LISA → [5]). And hence, those theories (typically where $\frac{\Lambda}{v} \leq 1$ and α_v is on the lower end), are more favorable... PROVIDED $\alpha_{latent} < 1$.

It should be said that finding out the gravitational wave power spectra from the parameters α_{latent} and $\frac{\beta}{H}$, is very difficult. People working at LISA have come up with ways of doing this, and have plotted the expected sensitivities of their detectors as $\frac{\beta}{H}$ - α_{latent} contours. These contours are dependent on nucleation temperature. To illustrate this, I have filtered out the above data, such that the theories have nucleation temperature between 200-400 GeV (and chose average nucleation temperature as 300 GeV). {Note that the example theory worked on in Section 4, fits this range}.



α_v Values	Colour Code	Λ/v Values	Symbol Code
0.51	Red	$\Lambda/v = 1/4$	Plus
0.54	Orange	$\Lambda/v = 1/2$	Downward triangle
0.57	Yellow	$\Lambda/v = 2/3$	Star
0.6	Green	$\Lambda/v = 1$	Circle
0.64	Cyan	$\Lambda/v = 3/2$	Diamond
0.65	Teal Blue	$\Lambda/v = 2$	Upward triangle
0.68	Navy Blue	$\Lambda/v = 4$	Cross
0.72	Indigo		
0.75	Fuchsia		
0.78	Pink		
0.81	Brown		

$v = 1000 \text{ GeV}$

Figure 13: Filtered data of Figure 12 such that their nucleation temperature is between 200-400 GeV

This was put through the PTPlot software, created by the LISA group (see reference [5]), to generate the plot below.

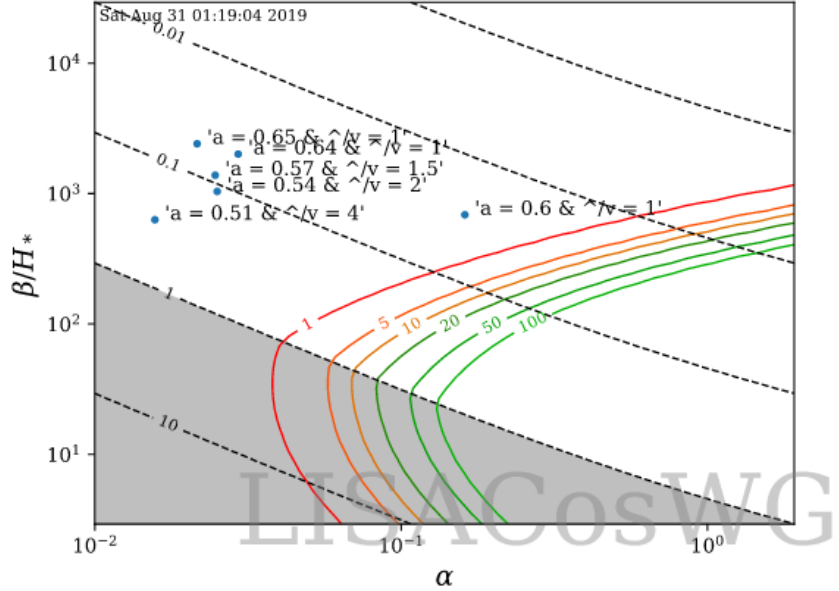


Figure 14: Plotted points are relevant data points from Figure 13 (the points are tagged with their α_v and Λ/v for $v = 1000$ GeV). Each of the coloured contours demarcate different sensitivities of of LISA [5]. Note that NONE of the points we came up with, are within the sensitivities of LISA.

And in this manner, my work got us all the way across Stage 2 of the flow-chart (Figure 1), with Figure 14 being a glimpse into the next stage of the process.

6 Appendix

6.1 Types of Potentials and different possible Instanton Solutions

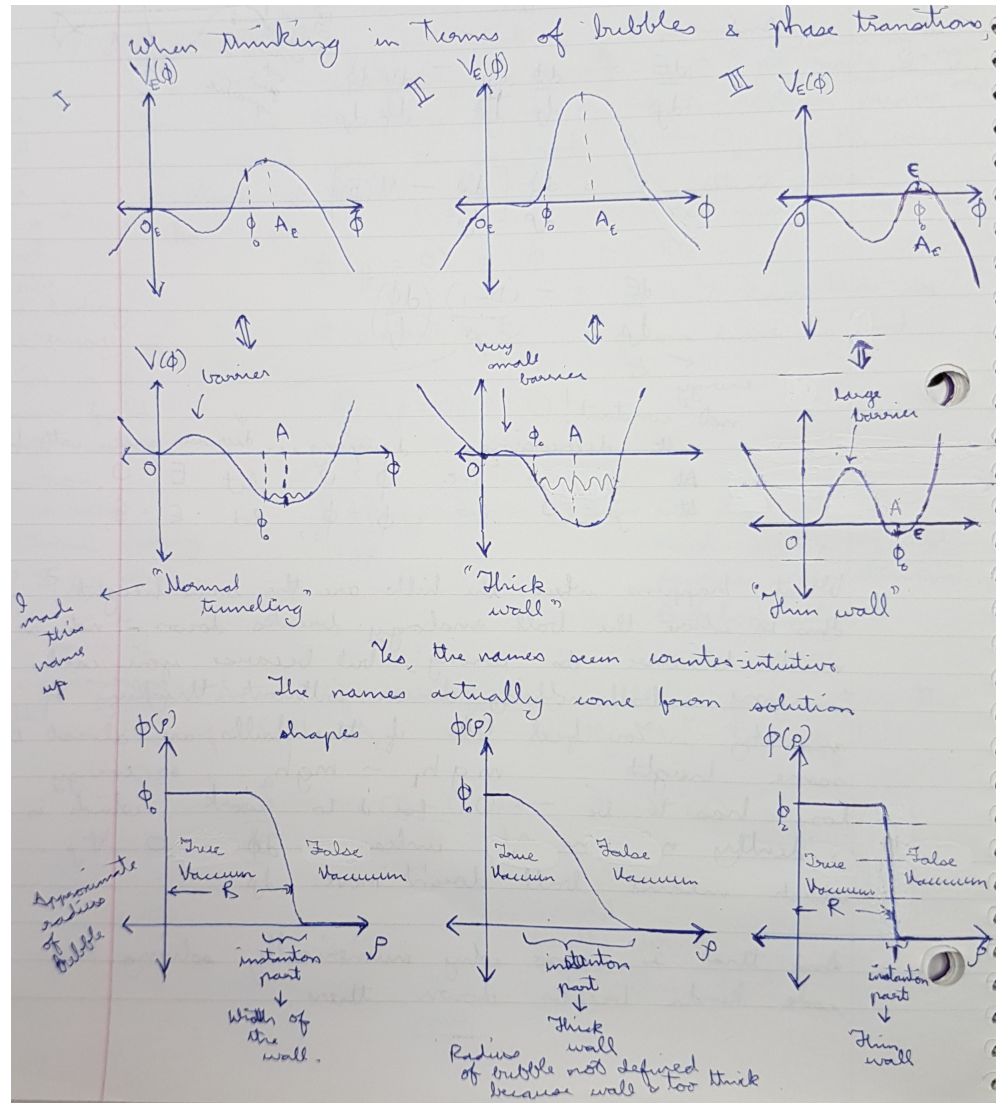


Figure 15: Different types of potentials and respective solutions

Note how as $\alpha_{v,eff} \rightarrow 0.5$, $\phi(r)$ resembles a step function with radius $\rightarrow \infty$.

6.2 The WKB Approximation

6.2.1 Theory and Context

First, we attempt to analyze the time-independent Schrodinger's equation:

$$-\frac{\hbar^2}{2m} \frac{d^2\psi}{dx^2} + V(x)\psi(x) = E\psi(x)$$

for the potential:

$$\begin{aligned} V(x) &= \infty & x < 0 \\ &= \mu^2 x^2 - Ax^3 + \lambda x^4 & x > 0 \end{aligned}$$

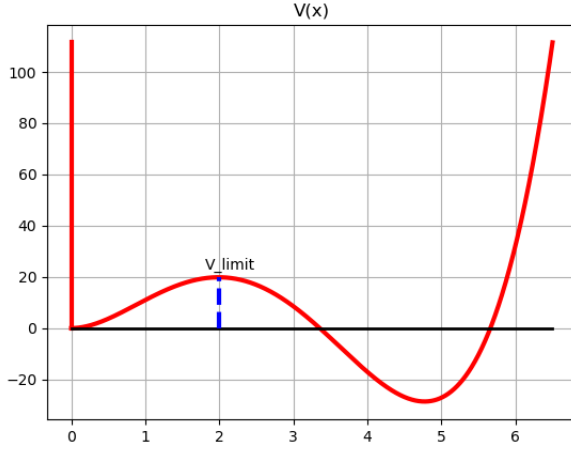


Figure 16: Quartic potential WKB Approximation

We simplify this into:

$$\frac{d^2\psi}{dx^2} = -\frac{p(x)^2}{\hbar^2} \psi(x)$$

— Eqn. 1

where,

$$p(x) = \sqrt{2m(E - V(x))}$$

Note how this resembles the form of the 2nd order differential equation used to describe the Simple Harmonic Oscillator's motion, if $p(x)$ were a constant. So... let us make the ansatz that:

$$\psi(x) = A(x)e^{i\phi(x)}$$

— Eqn. 2

where,

$$\phi(x) = \frac{1}{\hbar^2} \int p(x) dx$$

This makes intuitive sense, as this resembles the general solution to the equation of motion of the Simple Harmonic Oscillator, except with variable amplitude and frequency.

For this to solve our equation however, we need to make the following assumptions:

1. $\frac{A''(x)}{A} \rightarrow 0$
2. $A(x)$ must be real

Assumption 1 is valid only if $V(x)$ varies SLOWLY with position (especially in the regions where $E \approx V(x)$). THIS IS WORKABLE FOR OUR POTENTIAL (and all polynomial potentials).

Assumption 2 is convenience that makes finding probability densities a lot simpler, and makes intuitive sense (as the amplitude analogue).

These assumptions have the following implications:

1. $A(x) = \frac{C}{\sqrt{p(x)}}$, where C is the normalization constant
2. $\phi(x) = \frac{1}{\hbar} S(x)$ i.e. $S(x) = \int p(x) dx$, where $S(x)$ is the classical action
3. The WKB approximation is a semi-classical theory

Implication 1 falls directly from plugging in Eqn. 1 into the Schrodinger's equation, applying Assumption 1 and 2 and comparing the imaginary and real parts of the resulting expression.

Implication 2 and 3 are results of plugging in Eqn. 1 into the Schrodinger's equation, applying Assumption 1 and rearranging the expression to find:

$$H(x, \frac{d\phi}{dx}) = E$$

which, when comparing with the Hamilton-Jacobi, Time Independent equation (A CLASSICAL Equation), results in Implication 2. Also, when you work through the math of further, you find that Assumption 1 directly implies neglecting terms with higher powers of \hbar , in the exponent. This is because we are implicitly saying that $S(x) \gg \hbar^2 \Rightarrow$ a semiclassical theory (Implication 3).

Finally, the restriction on $V(x)$ means we can assume that for $E \gg V(x)$, the solution propagates *like* a sine wave ($p(x)$ near constant; purely real) and

for $E \ll V(x)$, the solution decays *like* an inverse exponential function i.e. TUNNELS ($p(x)$ near constant; purely imaginary). For both cases, since $p(x)$ near constant, we have the Analytic solution for it (directly using Eqn. 2). And for E comparable to $V(x)$, we do the following:

Let x_0 be the turning point i.e. where $V(x_0) = E$.

Expanding $V(x)$ as a Taylor series around x_0 :

$$V(x) = V(x_0) + V'(x_0)(x - x_0) + \frac{V''(x_0)}{2!}(x - x_0)^2 + \dots$$

Neglecting higher order terms, since we are near x_0 :

$$V(x) \approx E + V'(x_0)(x - x_0)$$

Now, Eqn. 1 boils down to the Airy Equation, which, again, we know the Analytic solution for. Since the wavefunction must be continuous, we have to connect all 3 kinds of regions together, carefully applying boundary conditions along the way. This will result in the final wavefunction that needs to be normalized to find C (refer Implication 1). And there you have it - we have the prescription to find a closed form Analytic solution to problems like the one we have.

Now let us look at our potential:

$\phi(x) = \frac{1}{\hbar} \int p(x)dx$ ends up being an elliptical integral... and so even the analytic solution, requires an element of numerical solving.

Apart from that, there are 2 cases: 1. Where $E > V_{limit}$ (Refer Figure 17); 2. Where $E < V_{limit}$ (Refer Figure 19).

6.2.2 Case 1: $E > V_{limit}$

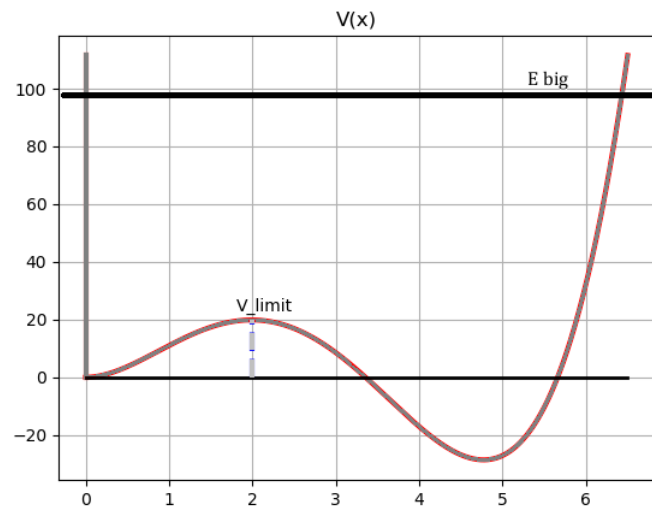


Figure 17: When $E > V_{limit}$

$\hookrightarrow E \text{ big}$ $x_1 = 0, x_2 = x_0, V(x) = \infty : x < 0,$
 \Rightarrow single potential well. Recalling previous work.

$$\psi(x) = 0 \quad x < 0$$

$$\psi_{\text{Patch with}} = \frac{2B}{\sqrt{1/p(x)}} \sin \left[\frac{1}{\hbar} \int \frac{1}{p(x')} dx' + \frac{\pi}{4} \right] \quad 0 < x < x_0$$

$$= \frac{B}{\sqrt{1/p(x)}} e^{-\frac{1}{\hbar} \int_x^{x_0} |p(x')| dx'} \quad x > x_0$$

Since $\psi(x)$ is continuous throughout & $B \neq 0$

At $x=0$,

$$\sin \left[\frac{1}{\hbar} \int_0^{x_0} |p(x')| dx' + \frac{\pi}{4} \right] = 0$$

$\hookrightarrow B = 0$ is trivial soln.

$$\frac{1}{\hbar} \int_0^{x_0} |p(x')| dx' + \frac{\pi}{4} = n\pi$$

$$\Rightarrow \int_0^{x_0} |p(x')| dx' = (n - \frac{1}{4})\hbar$$

$$\int_0^x |p(x')| dx' + \int_x^{x_0} |p(x')| dx' = (n - \frac{1}{4})\hbar$$

Figure 18: Analytic equations for $E > V_{limit}$

6.2.3 Case 2: $E < V_{limit}$

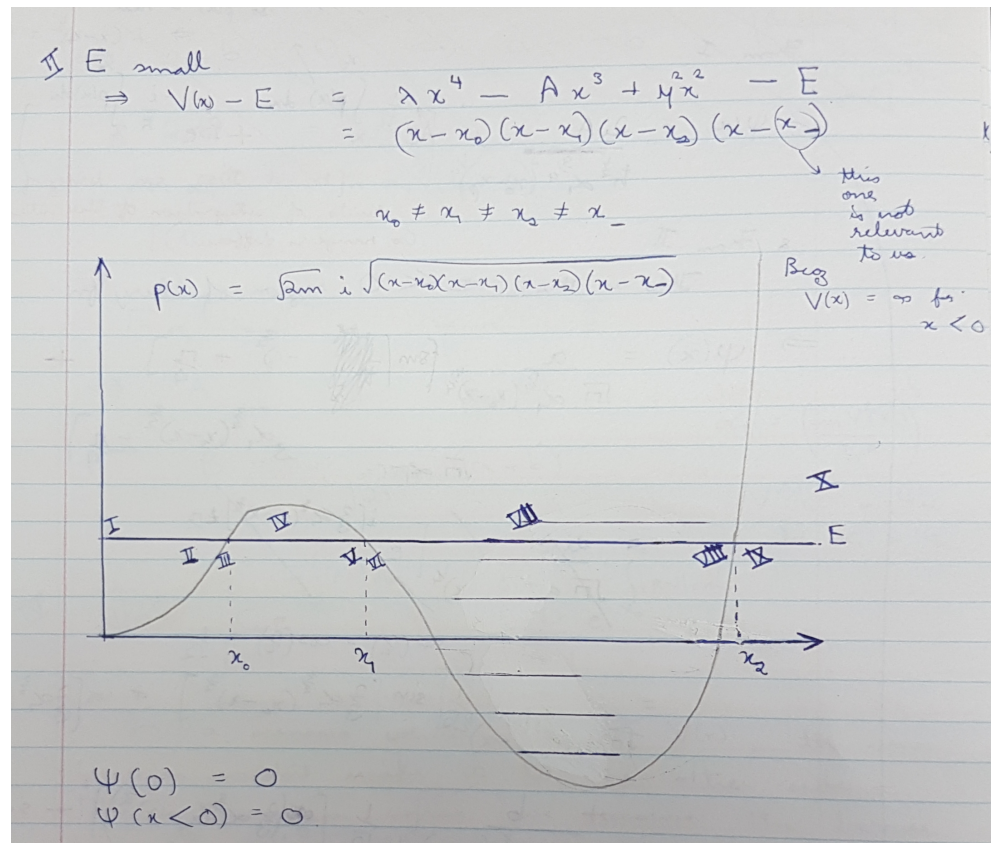


Figure 19: When $E < V_{limit}$

For E "small" :

$$x < x_0 \quad \psi(x) = \frac{1}{\sqrt{|p(x)|}} \sqrt{\frac{\alpha}{\pi}} \alpha \sin \left(\frac{1}{\hbar} \int_x^{x_0} p(u) du + \frac{\pi i}{4} \right)$$

$$[III \cap IV] - \psi(x) = \alpha \text{Ai}(\alpha_1(x-x_0)) - \frac{1}{\hbar} \int_x^{x_0} p(u) du$$

$$x_0 < x < x_1 \quad \psi(x) = \frac{1}{\sqrt{|p(x)|}} \frac{1}{2} \sqrt{\frac{\alpha}{\pi}} \alpha e^{-\frac{i\theta}{\hbar} \int_{x_0}^x p(u) du} = \frac{1}{\sqrt{|p(x)|}} \frac{1}{2} \sqrt{\frac{\alpha}{\pi}} \alpha \Gamma e^{\frac{i\theta}{\hbar} \int_{x_0}^x p(u) du}$$

$$[V \cap VI] - \psi(x) = \sqrt{\frac{\alpha_1}{\alpha_2}} \alpha \Gamma \text{Bi}(\alpha_2(x-x_1))$$

$$x_1 < x < x_2 \quad \psi(x) = \frac{1}{\sqrt{|p(x)|}} \sqrt{\frac{\alpha_2}{\pi}} \alpha \Gamma \cos \left(\frac{1}{\hbar} \int_{x_1}^x p(u) du + \frac{\pi i}{4} \right) = \frac{1}{\sqrt{|p(x)|}} \sqrt{\frac{\alpha_2}{\pi}} \alpha \Gamma e^{\frac{i\theta}{\hbar} \int_{x_1}^x p(u) du + \frac{\pi i}{4}}$$

$$[VII \cap VIII] - \psi(x) = \sqrt{\frac{\alpha_2}{\alpha_3}} e^{\frac{i\theta}{\hbar} \int_{x_2}^x p(u) du} \alpha \Gamma \text{Ai}(\alpha_3(x-x_2))$$

$$x > x_2 \quad \psi(x) = \frac{1}{\sqrt{|p(x)|}} \frac{1}{2} \sqrt{\frac{\alpha_3}{\pi}} e^{\frac{i\theta}{\hbar} \int_{x_2}^x p(u) du} \alpha \Gamma e^{-\frac{i\theta}{\hbar} \int_{x_2}^x p(u) du}$$

where:

$$\alpha_1 = \left(\frac{2m|V'(x_0)|}{\hbar^2} \right)^{1/3} \quad \alpha_3 = \left(\frac{2m|V'(x_2)|}{\hbar^2} \right)^{1/3}$$

$$\alpha_2 = - \left(\frac{2m|V'(x_1)|}{\hbar^2} \right)^{1/3} \quad \Gamma = e^{-\frac{i\theta}{\hbar} \int_{x_1}^{x_2} p(u) du}$$

$$\theta = (n'-1)\pi \quad V(x) = \lambda x^4 - A x^3 + \frac{1}{4} \lambda^2 x^2$$

(PTO).

$$\Rightarrow V'(x) = 4\lambda x^3 - 3Ax^2 + \frac{1}{2} \lambda^2 x$$

$$\Rightarrow E < V(x_{\text{limit}})$$

$$x_{\text{limit}} = 3A - \frac{\sqrt{9A^2 - 32\lambda^2}}{8\lambda}$$

$$p(x) = \sqrt{2m(E-V(x))}$$

$$\int_0^{x_0} p(x) dx = (n-\frac{1}{4})\pi \hbar \quad ; \quad \int_{x_1}^{x_2} p(x) dx = (n'-1)\pi \hbar.$$

Figure 20: Analytic equations for $E < V_{\text{limit}}$

6.2.4 Numerical vs. Analytic solutions:

Example shown: $V(x) = 19x^2 - 9.0177x^3 + x^4$

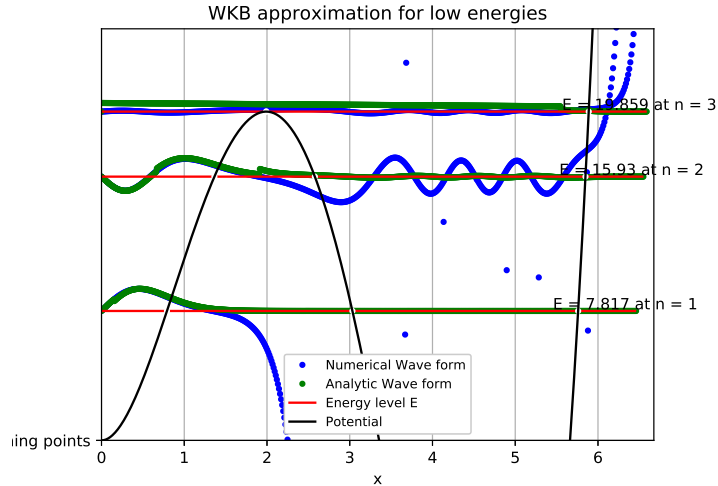


Figure 21: Numerical vs. Analytic solutions for $E > V_{limit}$

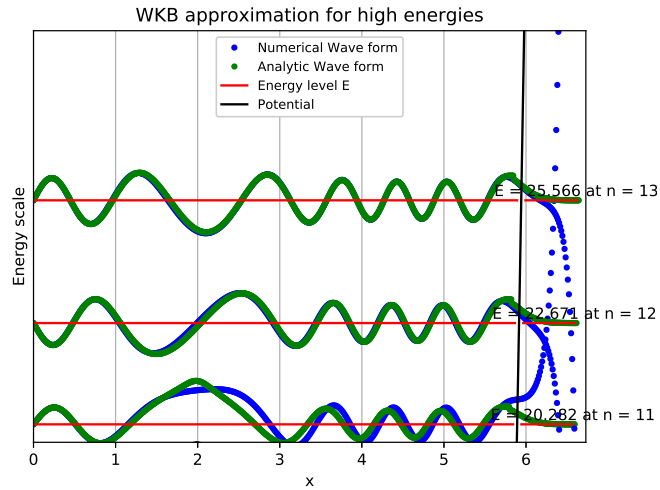


Figure 22: Numerical vs. Analytic solutions for $E < V_{limit}$

Note how the numerical solution breaks down near turning points and how the analytic solution is questionable when $E = V_{limit}$.

6.2.5 Inferences

Issues of note:

1. This is only for 1 dimension - multiple dimensions becomes very difficult to work with under this approximation
2. This is purely non-relativistic - we cannot work in the Minkowski space here
3. Analytic solution is highly dependent on potential and is hence difficult to modify when working with, say, temperature/time dependent potentials

Overall, the WKB approximation is not directly useful to the problems we will eventually face... but it does build up an intuition towards the fact that even in quantum scales, semiclassical approaches are often effective. Also, since we are in the realm of Quantum mechanics (as opposed to Quantum field theory) tunneling can be illustrated pretty easily, and helps build an intuition for when/where we would expect tunneling in Quantum field theory. Also, it is helpful to see the limitations of numerical solutions, and be able to compare and contrast it with analytic solutions - it is rare to find purely analytic solutions moving forward.

Refer [2][[3]; Notes 7, Appendix B].

References

- [1] Coleman, S.; "Fate of the False Vacuum I: Semi Classical Theory", 1977; Physics Review D, Vol.15, No.10
- [2] Griffiths, D.J.; Introduction to Quantum Mechanics, 1st edition, Chapter 8; Prentice Hall Inc.
- [3] Littlejohn, R.; Lecture Notes for 221A & 221B, 2018-19, UC Berkeley.
- [4] Tong, D.; Lecture Notes for Cosmology, 2019, University of Cambridge.
- [5] Weir, D. et.al.; "Science with the space-based interferometer eLISA. II: Gravitational waves from cosmological phase transitions", 2016; arXiv1512.06239; Also refer <http://www.ptplot.org/ptplot/>
- [6] Lancaster and Blundell; Quantum Field Theory for the Gifted Amateur, Chapter 50; Oxford University Press

Also refer to my code: <https://github.com/karishmamoothy/TRIUMF-2019-Summer.git>

